Modular Mutagenesis of Exons 1, 2, and 8 of a Glutathione *S*-Transferase from the Mu Class. Mechanistic and Structural Consequences for Chimeras of Isoenzyme 3–3[†,‡]

Pinghui Zhang,[§] Suxing Liu,[§] Shu-ou Shan,[§] Xinhua Ji,[§,∥] Gary L. Gilliland,[*,∥,⊥] and Richard N. Armstrong[*,§]

Department of Chemistry and Biochemistry, University of Maryland, College Park, Maryland 20742, Center for Advanced Research in Biotechnology of the Maryland Biotechnology Institute, University of Maryland, Shady Grove, and National Institute of Standards and Technology, 9600 Gudelsky Drive, Rockville, Maryland 20850

Received May 26, 1992; Revised Manuscript Received July 22, 1992

ABSTRACT: Exons 1 and 2 and exon 8 of the mu class GSH transferases from rat encode sequence-variable regions 1 and 4 of mu class isoenzymes, respectively. These two of four variable regions are located at the N- and C-termini of this isoenzyme class and impinge on the active site. In order to assess the influence of these variable regions on the catalytic diversity of the class mu isoenzymes, seven chimeric isoenzymes were constructed by transplantation of the variable regions of the sequence of the type 4 subunit into the corresponding regions of the type 3 subunit. The chimeric isoenzymes exhibit unique catalytic properties. Replacement of all, or part, of variable region 4 of the type 3 subunit with that of the type 4 subunit results in chimeric catalysts with higher turnover numbers in nucleophilic aromatic substitution reactions. Analysis of the crystal structure of isoenzyme 3–3 [Ji, X., Zhang, P., Armstrong, R. N., & Gilliland, G. L. (1992) *Biochemistry* (preceding paper in this issue)] suggests that interaction of the flexible C-terminal tail with the N-terminal domain helps limit the rate of product release from the active site of isoenzyme 3–3 in this type of reaction. Substitution of all, or part, of the sequence-variable region 1 of subunit 3 with that of subunit 4 results in chimeric isoenzymes that mimic the high stereoselectivity but not the catalytic efficiency of isoenzyme 4–4 toward α,β-unsaturated ketones. Modular mutagenesis of the N-terminal variable region together with linear free energy relationships using para-substituted 4-phenyl-3-buten-2-ones and the crystal structure of isoenzyme 3–3 has allowed the rapid location of a mutation, V9I, which appears to be crucial in determining the stereoselectivity of the chimeras and, by implication, isoenzyme 4–4 toward phenylbutenones and arene oxides.

The glutathione *S*-transferases are a family of enzymes that catalyze the addition of glutathione to lipophilic substrates bearing electrophilic functional groups. The cytosolic enzymes found in mammalian species are dimeric proteins with subunits that appear to be organized into four principal gene classes designated alpha, mu, and pi (Mannervik et al., 1985) and theta (Meyer et al., 1991). Both homo- and heterodimeric holoenzymes are found within a gene class but inter-gene-class heterodimers are not known. The cytosolic enzymes along with a genetically distinct microsomal enzyme are the principal catalysts involved in the initiation of the metabolism of endogenous and xenobiotic alkylating agents. As a group the enzymes catalyze the addition of GSH[1] to a very broad spectrum of substrates. Much of the catalytic diversity of the GSH transferases can be attributed to the existence of a large number of structurally distinct subunits. Although individual isoenzymes tolerate a remarkably wide range of substrates, each subunit type exhibits distinct preferences toward both the size and shape of the substrate and the type of electrophilic group. For recent reviews the reader is referred to Mannervik and Danielson (1988), Pickett and Lu (1989), and Armstrong (1991).

Examples of intra-gene-class differences in substrate preference can be seen in a comparison of the catalytic characteristics of isoenzymes 3–3 and 4–4 from the mu gene class of rat. Isoenzyme 3–3, for example, is better at catalyzing nucleophilic aromatic substitution reactions (Graminski et al., 1989). However, isoenzyme 4–4 is significantly better in catalyzing the addition of GSH to oxiranes and α,β-unsaturated ketones and exhibits a very high degree of stereoselectivity toward both (Cobb et al., 1983; Boehlert & Armstrong, 1984; Kubo & Armstrong, 1989). Furthermore, linear free energy relationships suggest that the stereoselectivity of isoenzyme 4–4 toward α,β-unsaturated ketones is influenced by electronic stabilization of one of the two possible diastereomeric transition states by the active site (Kubo & Armstrong, 1989). Whether this isoenzyme has an inherent steric preference for one transition state over the other is not known. In general, none of the structural bases for the differences in the catalytic behavior of these two isoenzymes have been elucidated.

Subunits of mu class isoenzymes from rat (e.g., subunit types 3, 4, and 6) are 217 residues in length and share a high (78%) overall sequence identity. Most of the sequence variation appears to be clustered in four regions of the primary structure as illustrated in Figure 1. The variable region located at the amino termini of the mu class isoenzymes (residues 1–33) exhibits relatively high (70%) sequence identity and is encoded by exons 1 and 2 of the genes as illustrated in Figure 1. The other three variable regions, contained in the

[†] This work was supported by a grant from the National Institutes of Health (GM 30910).

[‡] The crystallographic coordinates have been deposited in the Brookhaven Protein Data Bank under the file name 1GST.

* Address correspondence to these authors.

[§] University of Maryland, College Park.

[∥] Center for Advanced Research in Biotechnology.

[⊥] National Institute of Standards and Technology.

[1] Abbreviations: GSH, glutathione; CDNB, 1-chloro-2,4-dinitrobenzene; PBO, 4-phenyl-3-buten-2-one; XPBO, para-substituted 4-phenyl-3-buten-2-ones; PO, phenanthrene 9,10-oxide.

0006-2960/92/0431-10185$03.00/0

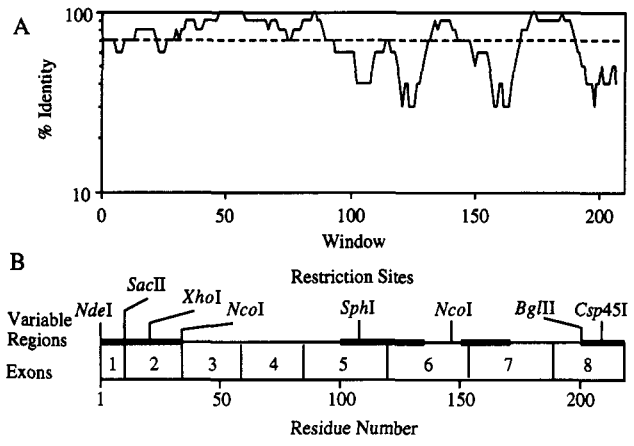

FIGURE 1: (A) Sequence identities of the mu class subunit types 3, 4, and 6 from rat. The sequences of the three subunits (Ding et al., 1986; Lai et al., 1986; Lai & Tu, 1986; Abramovitz & Listowsky, 1987) were aligned and scanned in one-residue increments with a ten-residue window. The percent identity (log scale) is plotted for each window. The log scale is used simply to highlight the four variable regions and has no theoretical significance. An arbitrary sequence identity of ≤70% (dotted line) is used to define a "variable" region. (B) Relative locations of the variable regions and the exon boundaries (Lai et al., 1988; Pickett & Lu, 1989) of the mu class isoenzymes and the restriction sites in the coding region of pGT33MX used for the construction of chimeric expression vectors. The locations of variable regions 1–4, as defined in panel A, are highlighted in bold from left to right.

C-terminal half of the protein, exhibit, on average, sequence identities of <50%. One region (residues 98–135) is encoded by a combination of exons 5 and 6 while the other two (residues 150–172 and 198–217) are encoded by exon 7 and exon 8, respectively (Figure 1). It is expected that the features which distinguish the catalytic properties of one mu class isoenzyme from another derive from structural elements contributed by one or more of these variable regions.

The regions of primary structure that control catalytic behavior can be explored, in principle, by modular or regional mutagenesis through the construction of chimeric genes that encode hybrid isoenzymes. The general idea, which has been exploited with numerous enzymes in the last few years [for a recent review, see Armstrong (1990)], is to transplant a region of structure of one enzyme, which has distinct catalytic properties, into another and to look for the simultaneous transfer of the catalytic properties. The method provides for the rapid scanning of sequence space in search of residues that may influence catalysis. In preliminary work we recently demonstrated the feasibility of this technique for the exploration of structure–function relationships in the class mu GSH transferases. Substitution of very small pieces of sequence from the variable regions at the N-terminus or C-terminus of the type 4 subunit into the type 3 subunit results in hybrid enzymes with altered catalytic properties (Zhang & Armstrong, 1990). Although the structural consequences of the chimeric constructs were not known at the time, it seemed evident that the N- and C-terminal regions were close in three dimensions and that both influence the architecture of the active site sufficiently to affect catalysis. The three-dimensional structure of isoenzyme 3–3 shows this conclusion to be correct (Ji et al., 1992). In fact, it is true that at least part of three of the four variable regions converges on the active site.

In this paper we describe the construction and expression of seven chimeric GSH transferases in which exons 1, 2, and 8, encoding variable regions 1 and 4 located at the N- and C-termini of the type 3 subunit, have been replaced wholly or in part with the corresponding exonic regions from the type 4 subunit. Characterization of the resulting hybrid isoenzymes reveals that although the high stereoselectivity of the type 4 subunit toward arene oxides and α,β-unsaturated ketones is mimicked by several of the hybrids, the mechanistic basis for the high efficiency of the type 4 subunit is not. The results, interpreted in the context of the high-resolution three-dimensional structure of the parent isoenzyme 3–3, suggest that the side chain at position 9 (valine or isoleucine) of exon 1 is probably responsible for the stereoselective behavior of the N-terminal hybrids. In addition, mutations in both variable regions appear to affect catalysis of nucleophilic aromatic substitution reactions by enhancing the rate of product release.

MATERIALS AND METHODS

Construction of Chimeric Genes. Expression vectors encoding the chimeric proteins were constructed by manipulation of the expression plasmids pGT33 and pGT33MX which encode native isoenzyme 3–3[2] (Zhang & Armstrong, 1990; Zhang et al., 1991). The relative locations of the restriction sites in the gene used for the construction of the chimeric plasmids are shown in Figure 1. The expression plasmid pGT43/1 which encodes the chimeric subunit $4^{9}3^{208}$ was prepared by replacing the 30-base-pair cassette between the *Nde*I and *Sac*II restriction sites with a synthetic linker encoding the first nine amino acids of the type 4 subunit as previously described (Zhang & Armstrong, 1990). Later this plasmid was altered by direct substitution of the 595-base-pair fragment which lies between the *Sac*II and *Csp*45I restriction sites of pGT33MX. This introduced a unique *Xho*I restriction site in the middle of exon 2 and the double mutation N198K/C199S in exon 8. The variant plasmid was designated pGT43/1MX and encodes the chimeric subunit $4^{9}3^{208}$ containing the above mentioned mutations. A plasmid encoding the chimeric subunit $4^{19}3^{198}$ was constructed by removal of the 28-base-pair cassette lying between the *Sac*II–*Xho*I restriction sites of pGT43/1MX and substitution of a synthetic linker corresponding to the sequence of subunit 4. This plasmid was designated pGT43/2MX. Complete replacement of exon 2 was accomplished after removal of the 36-base-pair cassette encoding residues 22–33 by partial digestion of pGT43/2MX with *Nco*I followed by cleavage with *Xho*I and ligation of a linker corresponding to the sequence of subunit 4. The resulting vector, designated pGT43/3MX, encodes the chimeric subunit $4^{33}3^{184}$ in which both exons 1 and 2 have been replaced.

Substitution of exon 8 was accomplished in two steps. The 627-base-pair fragment between the *Nde*I and *Csp*45I sites of plasmid pGT434/1 (Zhang & Armstrong, 1990), which encodes the chimeric subunit $4^{9}3^{200}4^{8}$, was replaced with the same fragment derived from pGT33MX. This plasmid, which encodes the chimeric subunit $3^{209}4^{8}$, is designated pGT34/2MX.[3] Construction of the expression plasmid pGT34/3X which encodes the chimeric subunit $3^{194}4^{23}$ was done by ligation of three fragments, the 5.0-kilobase-pair fragment flanked by the *Csp*45I and *Sac*II sites and the 545-base-pair fragment between the *Sac*II and *Bgl*II derived from separate digestions

[2] Two variants of the type 3 subunit have been reported (Ding et al., 1985; Lai et al., 1986). The variant encoded by pGT33 has Asn and Cys at positions 198 and 199. These positions are Lys and Ser in the protein encoded by pGT33MX (Zhang et al., 1991) as well as in the type 4 subunit. The N198K/C199S mutations have no discernible effect on the catalytic properties of isoenzyme 3–3, an observation that is consistent with the location of the side chains on the surface of the protein more than 20 Å from the active site (Ji et al., 1992).

of pGT34/2MX and a synthetic 45-base-pair linker encoding residues 195–210 of subunit 4 flanked by *Bgl*II and *Csp*45I sites. The triple ligation circumvented the inconvenience created by the additional, *Bgl*II site in the noncoding region of the plasmid. The plasmid pGT434/2X encoding the tripartite chimeric subunit $4^{33}3^{161}4^{23}$ was constructed by removing the 323-base-pair cassette flanked by the *Nde*I and *Sph*I restriction sites from pGT34/3X with the corresponding cassette from pGT43/3MX. The relevant regions of each plasmid were sequenced to ensure that no unwanted mutations were introduced. DNA sequencing was performed with Sequenase version 2 from U.S. Biochemical Corp.[4] with the enzyme described by Tabor and Richardson (1989).

Construction of an Expression Vector for Isoenzyme 4–4. An expression plasmid for isoenzyme 4–4 was assembled in a very similar way to that previously described for pGT33 (Zhang & Armstrong, 1990). Most of the coding region for subunit 4 was excised from the cDNA clone pUC18-187C (Lai et al., 1988) by cutting the plasmid at the *Acc*I site located 68 base pairs downstream of the initiation codon and at the *Xba*I site about 360 base pairs downstream of the stop codon. The complete coding sequence of subunit 4 was reassembled by ligating the 959-base-pair *Acc*I–*Xba*I fragment to a synthetic linker encoding the missing N-terminal residues and flanked by *Nde*I and *Acc*I restriction sites, followed by directional cloning between the *Nde*I and *Xba*I restriction sites of pMG27NS. This expression plasmid is designated pGT44.

Expression of Hybrid Isoenzymes in Escherichia coli. Each hybrid enzyme was produced in *E. coli* strain M5219 that had been transformed with the appropriate chimeric expression plasmid. Expression and purification of the hybrid proteins were carried out essentially as described before (Zhang & Armstrong, 1990) except that the transformed cells were grown at 30 °C and expression was induced at 42 °C in enriched media [Terrific broth described by Tartof and Hobbs (1987)] using a 1.5-L VirTis Moduculture fermenter equipped with a baffle, an impeller, and an aerator. The fermenter provided a vigorously stirred well-aerated environment. Temperature regulation was provided by a Thermistemp Model 63RC temperature controller, a thermistor, and a 250-W infrared lamp. Isolated yields of native and hybrid enzymes ranged from 20 to 200 mg/L of culture. Both native and hybrid enzymes were expressed as soluble proteins in *E. coli* with no evidence for formation of inclusion bodies.

Kinetic Analysis. The catalytic activities of native and mutant enzymes toward 1-chloro-2,4-dinitrobenzene (CDNB) and 4-phenyl-3-buten-2-one (PBO) were determined as described by Kubo and Armstrong (1989) and Zhang and Armstrong (1990). All kinetic experiments were carried out at pH 6.5 and 25 °C. Kinetic constants k_{cat} and k_{cat}/K_m^{CDNB} were obtained from initial velocity measurements with a saturating concentration of GSH, usually 2 mM. The K_m^{GSH} were obtained in the enzyme-catalyzed reactions at a fixed concentration of CDNB of 100 μM. Each initial velocity was measured at lesat in triplicate, and the kinetic constants were derived by fitting the initial velocity data to a hyperbola with the program HYPER (Cleland, 1979). The concentrations of active sites used to calculate the k_{cat} and k_{cat}/K_m were determined from the ϵ_{280} calculated from the tryptophan and tyrosine content of each protein. Initial rates for reactions with the para-substituted PBO (XPBO) were obtained under the same conditions as described for CDNB except that considerable care was required to eliminate or account for the uncatalyzed reaction of GSH with the more electron deficient substrates (X = NO_2 or Br). The stereoselectivities of enzymes toward phenanthrene 9,10-oxide (PO) and XPBO were determined as described in Cobb et al. (1983) and Kubo and Armstrong (1989), respectively. Dissociation constants for GSH were determined at pH 7.0 by the fluorescence titration procedure previously described (Zhang & Armstrong, 1990).

Table I: Binding Constants for GSH and Kinetic Constants for the Enzyme-Catalyzed Additions of GSH to 1-Chloro-2,4-dinitrobenzene at pH 6.5

enzyme	K_d^{GSH} [a] (μM)	k_{cat} (s^{-1})	k_{cat}/K_m^{CDNB} (10^5 M^{-1} s^{-1})	K_m^{GSH} (μM)
3–3	21 ± 4	19 ± 1	4.0 ± 0.1	45 ± 4
4–4	24 ± 4	4.6 ± 0.2	0.21 ± 0.01	27 ± 4
$(4^{93}3^{208})_2$	42 ± 6	28 ± 2	0.89 ± 0.04	54 ± 8
$(4^{193}3^{198})_2$	18 ± 3	85 ± 4	1.87 ± 0.03	86 ± 5
$(4^{33}3^{184})_2$	39 ± 3	55 ± 2	1.48 ± 0.04	132 ± 9
$(3^{209}4^{8})_2$	50 ± 7	161 ± 10	1.91 ± 0.02	650 ± 80
$(3^{194}4^{23})_2$	12 ± 1	109 ± 5	1.39 ± 0.02	160 ± 16
$(4^{93}2^{00}4^{8})_2$	20 ± 3	78 ± 5	1.20 ± 0.03	210 ± 15
$(4^{33}3^{161}4^{23})_2$	11 ± 1	37 ± 1	0.23 ± 0.004	74 ± 2

[a] Determined by fluorescence titration at pH 7.0.

RESULTS

Expression, Purification, and Characterization of Chimeric Isoenzymes. All of the chimeric enzymes can be expressed in moderate to high yields in *E. coli* with the only notable caveat being that the yields of the N-terminal chimeras are usually much lower than either the native enzymes or the C-terminal chimeras. Purification of the proteins by affinity chromatography is unremarkable, and the enzymes appear to be stable to storage once purified. The enzymes behave as dimers on gel filtration chromatography with no evidence for formation of either active or inactive monomers. All of the chimeras retain the ability to bind GSH, though some modest differences are noticed in the dissociation constants determined by fluorescence titration (Table I). The actual mutations that result from the construction of the chimeric isoenzymes are shown in Figure 2. Altogether 19 mutations are introduced in the chimera $(4^{33}3^{161}4^{23})_2$ in which exons 1, 2, and 8 are replaced in their entirety.

Although the majority of the 19 mutations introduced into the chimera in which all of variable regions 1 and 4 are replaced result in the conservative replacement of a side chain, three (N8D, A195D, and T205K) introduce a change in charge, and five (I3T, T13A, S209A, Q213F, and N216P) alter the hydrophobic character of the side chain. Two of the mutations, L19F and L211M, involve side chains that are substantially buried. However, the mutations are conservative ones. Two mutations, P15A and N216P, may introduce a change in the backbone conformation. How these and the nine more conservative changes may affect the structure of the active site and hence catalysis is discussed in more detail below.

Kinetic Characteristics of the Chimeric Enzymes. The catalytic properties of the native (parent) and chimeric GSH

[3] The plasmid pGT34/2 originally reported (Zhang & Armstrong, 1990) was recently found to have a two-codon deletion corresponding to W214 and N215 in the short C-terminal portion of the sequence encoded by the synthetic linker. This discovery clearly points out the importance of sequencing the DNA in the coding portions of the expression vectors, even those parts derived from synthetic oligonucleotides.

[4] Certain commercial equipment, instruments, and materials are identified in this paper in order to specify the experimental procedure as completely as possible. In no case does such identification imply a recommendation or endorsement by the National Institute of Standards and Technology nor does it imply that the material, instrument, or equipment identified is the best available for the purpose.

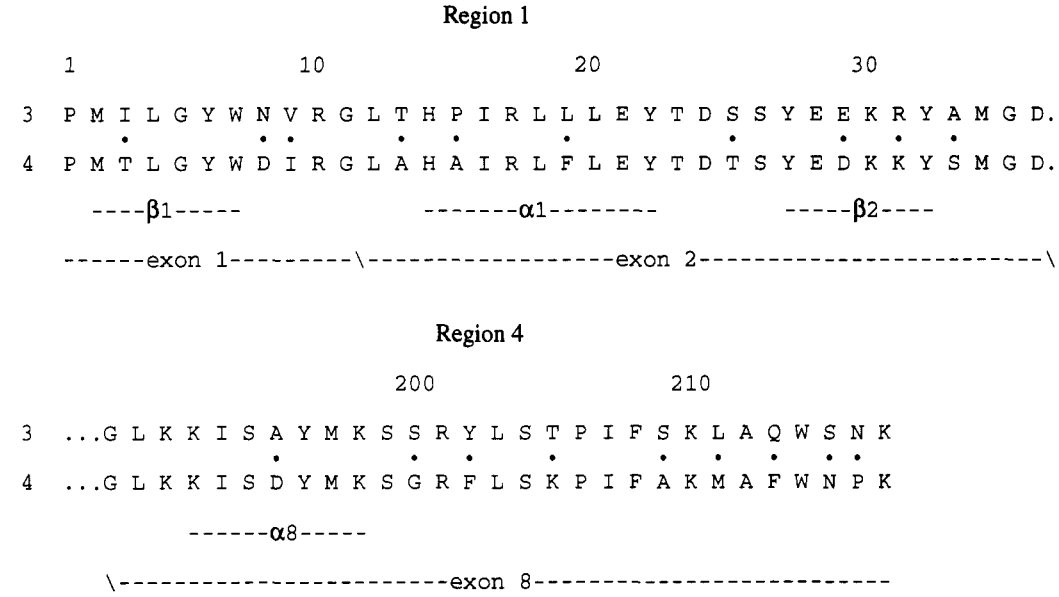

FIGURE 2: Sequence alignments of variable regions 1 and 4 of subunits 3 and 4 of the mu class GSH transferases from rat liver. The 19 differences in sequence between these two regions are highlighted with dots. The positions of major secondary structural elements with respect to the mutations are also noted.

transferases toward 1-chloro-2,4-dinitrobenzene are summarized in Table I. It has been known for some time that isoenzyme 3–3 is significantly more efficient than isoenzyme 4–4 at catalyzing nucleophilic aromatic substitution reactions. Therefore, the reaction of GSH with 1-chloro-2,4-dinitrobenzene can be used as an indicator of the degree of retention of the catalytic characteristics of the type 3 subunit in the hybrid isoenzymes. The data presented in Table I indicate that the modular mutations incorporated into the hybrid isoenzymes do not seriously impair their ability to catalyze the addition of GSH to CDNB. In fact, all of the chimeric isoenzymes exhibit turnover numbers (k_{cat}) that are greater than that of isoenzyme 3–3 and in this way resemble isoenzyme 3–3 more closely than isoenzyme 4–4. However, the efficiency of the modular mutants as judged by k_{cat}/K_m^{CDNB} lies somewhere between the extremes of the two parents. The observed K_m^{GSH} for several of the chimeras are substantially greater than those observed for the parents and quite different than K_d^{GSH} determined by fluorescence titration. It is clear that K_m^{GSH} is a kinetically complex term in this reaction and not an accurate reflection of the binding of GSH.

The fact that isoenzyme 4–4 is more efficient and stereoselective toward α,β-unsaturated ketones can be exploited as a signal to monitor the transfer of the catalytic properties of the type 4 subunit into the chimeric proteins. The kinetic constants for the enzyme-catalyzed addition of GSH to 4-phenyl-3-buten-2-one are summarized in Table II. It is obvious from these data that, in spite of the substitutions of the primary structure of the type 4 subunit into the framework of the type 3 subunit, none of the hybrid isoenzymes has a significantly enhanced catalytic efficiency toward the enone substrate. The marginal increases in either k_{cat} or k_{cat}/K_m^{PBO} are, in any case, less than a factor of 3.

Stereoselectivity of the Chimeric Isoenzymes. Another criterion for the transfer of the catalytic character of the type 4 subunit into the chimeric isoenzymes is the high degree of stereoselectivity exhibited by this subunit toward both 4-phenyl-3-buten-2-one (**1**, X = H) and phenanthrene 9,10-oxide, the reactions of which are illustrated in Scheme I. The stereoselectivities of the chimeric isoenzymes toward both of these substrates are given in Table II. All of the chimeric isoenzymes exhibit stereoselectivities that are significantly

Table II: Kinetic Constants and Relative Stereoselectivity of Native and Chimeric Enzymes toward 4-Phenyl-3-buten-2-one (PBO) and Absolute Stereoselectivity toward Phenanthrene 9,10-Oxide (PO)

			mol %	
enzyme	k_{cat} (s^{-1})	k_{cat}/K_m^{PBO} (10^3 M^{-1} s^{-1})	isomer A[a]	diastereomer[b] (9*S*,10*S*)
3–3	0.29 ± 0.01	3.0 ± 0.1	50 ± 3	43 ± 2
4–4	8.5 ± 0.7	48 ± 2	90 ± 1	≥99.5
$(4^{93}3^{208})_2$	1.40 ± 0.05	6.1 ± 0.1	93 ± 1	85 ± 2
$(4^{193}3^{198})_2$	1.19 0.05	6.5 ± 0.1	93 ± 1	93 ± 2
$(4^{333}3^{184})_2$	0.88 ± 0.06	5.8 ± 0.2	93 ± 1	92 ± 2
$(3^{209}4^{8})_2$	1.3 ± 0.1	4.6 ± 0.04	80 ± 1	77 ± 2
$(3^{194}4^{23})_2$	2.1 ± 0.4	4.3 ± 0.1	86 ± 1	85 ± 2
$(4^{93}3^{200}4^{8})_2$	0.95 ± 0.04	3.7 ± 0.04	75 ± 1	74 ± 2
$(4^{333}3^{161}4^{23})_2$	0.69 ± 0.04	3.9 ± 0.1	91 ± 1	89 ± 2

[a] Isomer A is defined as the first product that elutes from reversed-phase HPLC. The absolute configuration of this product has not been established. [b] From reaction with phenanthrene 9,10-oxide.

Scheme I

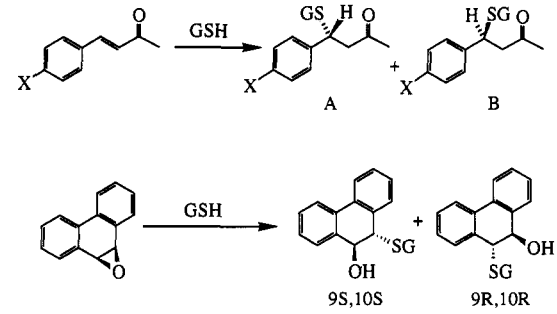

higher than the parent isoenzyme 3–3 and in some cases approach or exceed the stereoselectivity observed with isoenzyme 4–4. Although the catalytic efficiencies of the chimeras toward **1** are quite similar to the parent isoenzyme 3–3, the catalysts more closely resemble the parent subunit 4 when judged on the basis of their stereoselectivity. It is also interesting to note that each isoenzyme responds in a very similar manner to each of the two substrates, suggesting that the stereoelectronic demands of the transition states for both substrates are quite similar. Comparison of the stereoselectivities of the various hybrid isoenzymes toward **1** suggests that one crucial mutation influencing the stereoselectivity is

located in exon 1. Nevertheless, it is clear that both the N- and C-terminal variable regions influence the stereoselectivity of the proteins, sometimes in a noncooperative sense; compare, for example, $(4^93^{208})_2$ and $(4^93^{2004^8})_2$.

Substituent Dependence of the Michael Additions. The previously observed dependence of the kinetics and stereoselectivity of isoenzyme 4–4 on the electronic nature of the substituent in a series of para-substituted 4-phenyl-3-buten-2-ones (**1–5**) can be taken as evidence that the stereoselectivity of this isoenzyme is, at least in part, electronic in origin and related to the catalytic efficiency (k_{cat}/K_m) of the enzyme toward a particular substrate (Kubo & Armstrong, 1989). The apparent dissociation of the catalytic efficiency from the sereoselectivity that is manifest by the chimeric isoenzymes suggests that the stereoelectronic origin of these effects may be different. In order to more thoroughly evaluate the mechanistic basis of the stereoselectivity exhibited by the chimeras, the effect of substituent on the reaction of isoenzyme 3–3 and a representative chimeric isoenzyme with a high stereoselectivity was determined.

Previous work with isoenzyme 4–4 suggests that k_{cat}/K_m^{XPBO} follows the general linear free energy relationship shown in eq 1, where σ is the Hammett substituent constant, ρ_{app} is the

$$\log (k_{cat}/K_m^{XPBO}) - c_{app}\pi = \rho_{app}\sigma \qquad (1)$$

composite sensitivity of both transition states A‡ and B‡ to the electronic effect of the substituent, π is the Hansch hydrophobic parameter for the substituent, and c_{app} is a composite coefficient that measures the influence of the hydrophobic effect on partitioning the substrate between the ground state (free enzyme and substrate) and the two transition states. This linear free energy relationship for isoenzyme 4–4 from Kubo and Armstrong (1989) is illustrated in Figure 3, where $\rho_{app} = 0.93$ and $c_{app} = 0.43$ ($r^2 = 0.994$).

The dependencies of the kinetics of isoenzyme 3–3 and the chimera $(4^{193}3^{198})_2$ on the identity of the para substituent of substrates **1–5** are compared to those of isoenzyme 4–4 in Table III and Figure 3. It is clear that the more electron deficient (NO_2- and Br-substituted) substrates are better with both isoenzyme 3–3 and the chimera, as was found with isoenzyme 4–4. Moreover, the hybrid isoenzyme $(4^{193}3^{198})_2$ also follows the relationship expressed in eq 1 with $\rho_{app} = 1.76$ ($r^2 = 0.974$) when c_{app} is assumed to be 0.43. In contrast, log (k_{cat}/K_m^{XPBO}) for isoenzyme 3–3 appears to be rather poorly correlated with the Hammett substituent constant σ ($\rho_{app} = 1.23$, $r^2 = 0.878$). Although the linear correlation with σ is not as impressive as it is for isoenzyme 4–4 and the chimera, the trend in the data is quite obvious.[5] It is notable that both isoenzyme 3–3 and the chimera are much more sensitive ($\rho_{app} > 1.23$) to the electronic effect of the substituent than is isoenzyme 4–4 ($\rho_{app} = 0.93$).

The dependence of the stereoselectivity of the three isoenzymes on the Hammett substituent constant σ for this series of substrates is illustrated in Figure 3. The stereoselectivity of isoenzyme 4–4 follows the linear free energy relationship expressed in eq 2, where A and B are the two

$$\log ([A]/[B]) = (\rho_A - \rho_B)\sigma \qquad (2)$$

products and $\rho_{obs} = \rho_A - \rho_B$ measures the difference in sensitivity of the two transition states, A‡ and B‡, to the

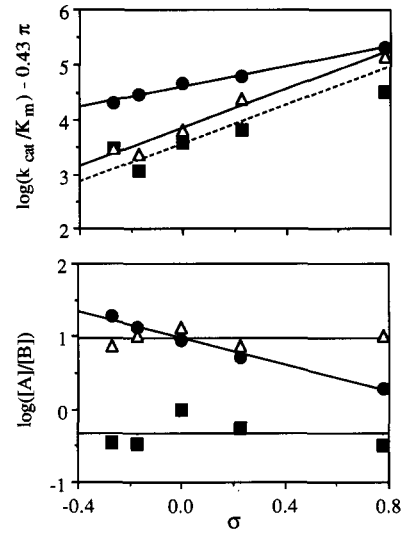

FIGURE 3: (Top panel) Dependence of kinetics of isoenzymes 4–4 (●) and 3–3 (■) and the chimeric isoenzyme $(4^{193}3^{198})_2$ (△) on the Hammett substituent constant σ. The solid lines are fits of the data to eq 1 in which c_{app} has been fixed at 0.43. Slopes and correlation coefficients of the lines for isoenzyme 4–4 and $(4^{193}3^{198})_2$ are $\rho_{app} = 0.93$, $r^2 = 0.994$ (Kubo & Armstrong, 1989) and $\rho_{app} = 1.76$, $r^2 = 0.974$, respectively. A least-squares line is not shown for isoenzyme 3–3 inasmuch as the correlation coefficient is <0.95. The broken line represents the calculated relationship between σ and log (k_{cat}/K_m^B) for transition state B‡ in the reaction catalyzed by isoenzyme 4–4, where $\rho_B = 1.74$, $r^2 = 0.994$ (Kubo & Armstrong, 1989). (Bottom panel) Dependence of the stereoselectivity of isoenzymes 4–4 (●) and 3–3 (■) and the chimeric isoenzyme $(4^{193}3^{198})_2$ (△) on the Hammett substituent constant σ. The solid line for isoenzyme 4–4 is a fit to the equation log ([A]/[B]) = $(\rho_A - \rho_B)\sigma$ with $\rho = -0.94$ and a correlation coefficient, r^2, = 0.994. The solid lines for isoenzymes 3–3 and $(4^{193}3^{198})_2$ represent the average log ([A]/[B]) for the series of substrates (e.g., $\rho_A - \rho_B = 0$). The values of σ and π for each substituent are H, 0.0, 0.0; NO_2, 0.78, –0.28; Br, 0.23, 0.86; CH_3, –0.17, 0.56; and CH_3O, –0.27, –0.02 and were obtained from Hansch and Leo (1979) and Fujita et al. (1964), respectively.

Table III: Kinetic Constants and Relative Stereoselectivities of Isoenzymes 3–3 and 4–4 and the Chimeric Isoenzyme $(4^{193}3^{198})_2$ with Para-Substituted 4-Phenyl-3-buten-2-ones

isoenzyme	substrate	substituent X	k_{cat} (s^{-1})	k_{cat}/K_m^{XPBO} (10^3 M^{-1} s^{-1})	mol % of isomer A[a]
4–4[b]	1	H	8.5 ● 0.7	48 ± 0.2	90 ± 1
	2	NO_2	22 ± 2.0	160 ± 10	66 ± 1
	3	Br	4.5 ± 0.3	150 ± 10	84 ± 1
	4	CH_3	4.7 ● 0.3	50 ± 0.2	93 ± 1
	5	OCH_3	2.2 ± 0.1	20 ± 0.1	95 ± 1
3–3	1	H	0.29 ● 0.01	3.0 ± 0.1	50 ± 3
	2	NO_2	0.79 ± 0.04	25 ± 2	24 ± 1
	3	Br	0.70 ● 0.06	16 ± 1	35 ± 1
	4	CH_3	0.16 ± 0.02	2.0 ● 0.07	25 ± 1
	5	OCH_3	0.18 ± 0.01	2.9 ± 0.1	26 ± 1
$(4^{193}3^{198})_2$	1	H	0.66 ● 0.02	6.7 ± 0.1	93 ± 1
	2	NO_2	3.4 ± 0.2	114 ± 8	91 ± 1
	3	Br	1.38 ● 0.03	58 ● 2	88 ± 1
	4	CH_3	0.39 ± 0.01	4.2 ± 0.1	91 ± 1
	5	OCH_3	0.28 ± 0.01	2.9 ± 0.1	88 ± 1

[a] The stereoselectivities are conservatively reported to two significant figures, and standard deviations of 1% or less are reported as 1%. [b] Data for isoenzyme 4–4 are from Kubo and Armstrong (1989).

[5] The reason for the poor correlation of k_{cat}/K_m^{XPBO} with σ for isoenzyme 3–3 is not obvious. The assumption that the influence of desolvation of the various substituents on partitioning of the substrates between aqueous solution and the transition state is similar for all three isoenzymes appears to be a good one since values of c_{app} other than 0.43 (established for isoenzyme 4–4) do not significantly improve the correlations for either isoenzyme 3–3 or the chimera. The poorer correlation seen with isoenzyme 3–3 appears to be due to the anomalous behavior of one substrate, **5**. Although the correlation can be much improved by excluding **5** from the analysis, there is no mechanistic or structural justification for doing so.

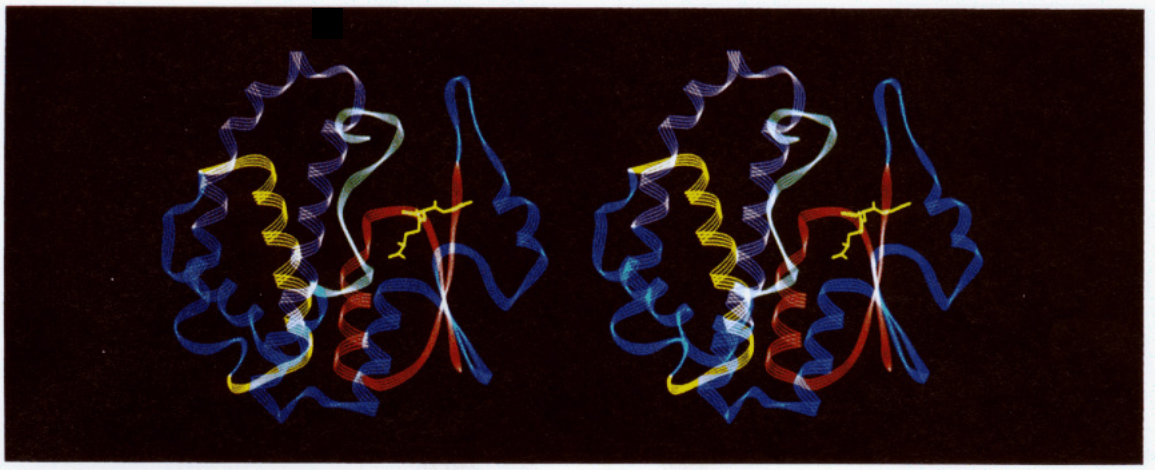

FIGURE 4: Stereoview of a ribbon diagram of one subunit of isoenzyme 3–3. The constant regions of sequence are shown in dark blue, and variable regions 1, 2, 3, and 4 are highlighted in red, purple, yellow, and light green, respectively. A stick model of glutathione is shown in yellow to indicate the location of the active site.

electronic effect of the substituent. The value of this relationship lies in the fact that it directly compares the two transition states and is free of the influence of ground-state effects such as the hydrophobicity of the substituent. The data of Figure 3 suggest that the two parallel transition states in the reaction catalyzed by isoenzyme 4–4 have very different sensitivities to the electronic nature of the substituent ($\rho_A - \rho_B = -0.94$, $r^2 = 0.994$) (Kubo & Armstrong, 1989). In contrast, isoenzyme 3–3 shows a much different stereoselectivity toward the same series of substrates which is not, in any simple way, dependent on the electronic effect of the substituent. To a first approximation it appears that $\rho_A - \rho_B \cong 0$. Isoenzyme 3–3 actually exhibits a higher stereoselectivity toward **2** as compared to **1** and prefers the transition state for formation of the B stereoisomer, a result which is just opposite to that seen with isoenzyme 4–4. In addition, the degree of discrimination by isoenzyme 3–3 between the two transition states with the more electron rich substrates (**3** and **4**) is much more modest than that exhibited by isoenzyme 4–4.

The chimeric isoenzyme $(4^{193}3^{198})_2$, which was chosen as representative of the highly stereoselective hybrid constructs, exhibits unique catalytic properties toward the substituted enones. It mimics isoenzyme 4–4 in that it catalyzes the Michael addition with a relatively high selectivity for formation of product diastereomer A with **1** but is unlike isoenzyme 4–4 inasmuch as the stereoselectivity is virtually independent of the para substituent. In fact, the stereoselectivity varies less than 5% across the whole range of substrates, as shown in Figure 3. In this case it is clear that $\rho_A - \rho_B = 0$.

DISCUSSION

Sequence-Variable Regions and the Active Site. A corollary to the proposition that the variable regions of sequence in the mu class isoenzymes are responsible for the differences in catalytic properties is that these regions of structure should be in the proximity of the active site. The three-dimensional structure of isoenzyme 3–3 indicates that side chains contributed by at least three of the four variable regions in the sequence impinge, to some extent, on the active site. This is particularly true of parts of regions 1, 2, and 4, as can be seen in Figure 4. This observation is interesting since it provides evidence that the evolution of catalytic diversity within a gene family has been focused on, though not necessarily limited to, modules of sequence that define the active site. Although side chains of variable region 3 come no closer than about 10 Å to the active site, the participation of variable regions 1, 2, and 4 in the architecture of the active site is obvious from the crystal structure of isoenzyme 3–3. Region 1 forms part of one wall in the active site beginning with Y6, the hydroxyl group of which participates in a hydrogen bond with the sulfur of GS^-, and continuing through the loop (residues 8–13) that connects the first β-strand (residues 2–7) to the first α-helix (residues 14–22). The relatively high sequence identity (70%) in region 1 is a consequence of the fact that it is intimately involved in the binding and activation of GSH. The structural elements that contribute to this function are expected to be conserved. The second variable region, which spans parts of the α4 and α5 helices located in the C-terminal domain of the protein, also contributes to the architecture of the substrate binding site. This involves the hydrophobic face of a section (residues 104–116) of the α4 helix which includes the side chains of M104, M108, I111, M112, and Y115. Finally, variable region 4 at the C-terminus of the protein is a relatively flexible, meandering tail that wraps across one face of the active site and touches the N-terminal domain of the subunit. Only one mutation (S209A) is within 9 Å of the sulfur of GSH in the active site. However, the key to the involvement of exon 8 in altering catalysis may lie in its flexibility and its mutual interactions with the other variable regions.

The proximity of the various mutations in exons 1 and 2 (variable region 1) and exon 8 (variable region 4) to the active site and to each other is shown in Figure 5. At least three direct contacts (<4.5 Å) between a mutated side chain of one of the two variable regions with the other region are apparent. Contacts between mutated residues in exons 1 and 8 with the opposing region include van der Waals interactions between the side chain of V9 (V9I mutation) and P206 and between Y202 (Y202F mutation) and H14. The side chain of R31 of the R31K mutation in exon 2 is in van der Waals contact with L203 and forms a hydrogen bond with the main-chain carbonyl of R201 of exon 8. The close proximity of the N- and C-terminal variable regions to each other and the active site is almost certainly responsible for their mutual influence on the catalytic properties of the chimeric isoenzymes.

Structural Effects on Nucleophilic Aromatic Substitution Reactions. The fact that isoenzyme 3–3 is more efficient (as manifest in k_{cat}/K_m^{CDNB}) than isoenzyme 4–4 at catalyzing nucleophilic aromatic substitutions has been attributed to its ability to stabilize the σ-complex intermediate in the reaction (Graminski et al., 1989). It is not readily apparent from the

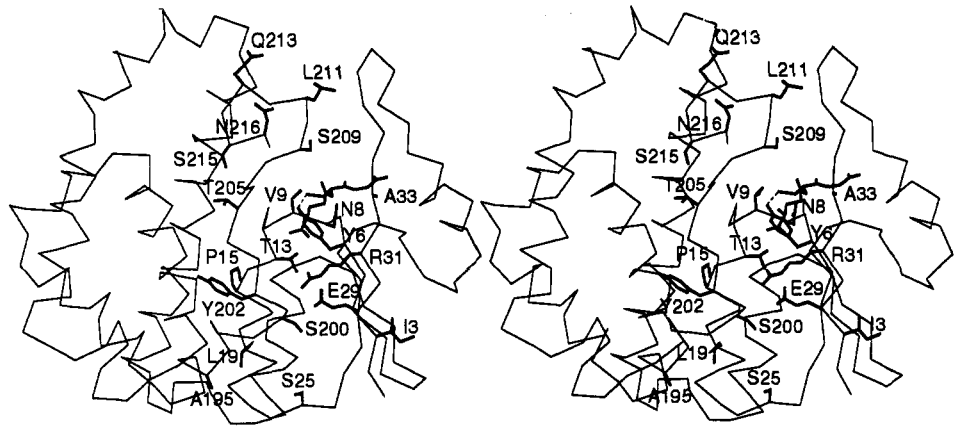

FIGURE 5: Stereoview of the α-carbon backbone (light lines) of subunit A of isoenzyme 3–3 with the side chains of the residues that are mutated in the construction of the chimeric isoenzymes highlighted in bold lines. The mutations are I3T, N8D, and V9I in exon 1; T13A, P15A, L19F, S25T, E29D, R31K, and A33S in exon 2; and A195D, S200G, Y202F, T205K, S209A, L211M, Q213F, S215N, and N216P in exon 8. The side chain of Y6 and glutathione are also illustrated with bold lines. The hydrogen bond between the hydroxyl group of Y6 and the sulfur of GSH is shown with a dashed line.

crystal structure why isoenzyme 3–3 should be more efficient. The lack of any obvious side chains that might aid in stabilization of the intermediate suggests that perhaps a secondary structural element such as the α1 helix, the dipole of which points at the active site, may be involved. That all of the chimeras, but one, $(4^{33}3^{161}4^{23})_2$, have efficiencies approaching that of native isoenzyme 3–3 suggests that the ability to stabilize the σ-complex is not perturbed by many of the multiple mutations. Why $(4^{33}3^{161}4^{23})_2$ is much less efficient is not clear. It appears that the decreased efficiency is one of the manifestations of the interaction between the N- and C-terminal variable regions since it is observed only when both regions are mutated. Moreover, the crucial structural change appears to involve the last half of variable region 1 (exon 2) and the first half of variable region 4 (exon 8) since $(4^{9}3^{200}4^{8})_2$ shows a relatively high k_{cat}/K_m^{CDNB}. Although there are no direct contacts between side chains of residues mutated in exons 2 and 8, the close proximity of a couple of the mutations in three dimensions leaves them suspect (Figure 5). For example, the Y202F mutation in exon 8 would result in loss of a hydrogen bond to a water molecule that is shared with the imidazole ring of H14. Although H14 is conserved in both parents, it is flanked by the T13A and P15A mutations in exon 2. In addition, the R31K mutation in exon 2 might result in the loss of the hydrogen bond between this side chain and the main-chain carbonyl of residue 201 in exon 8. It is certainly difficult to predict the net structural or electrostatic perturbation of these and other mutations on the active site. Inasmuch as H14 is located at the base of the α1 helix, which points directly at the active site, it is interesting to speculate that perhaps the combined mutations could realign the helix dipole and affect stabilization of the intermediate.

In contrast to k_{cat}/K_m, the turnover numbers of all the chimeric isoenzymes toward CDNB are greater than that for isoenzyme 3–3. Preliminary studies of the rate of release of 1-(*S*-glutathionyl)-2,4-dinitrobenzene from the active site of isoenzyme 3–3[6] and the fact that the turnover number is independent of pH (Liu et al., 1992) provide strong evidence that *the rate-limiting step in the turnover of this particular substrate with isoenzyme 3–3 is product release.* The increased turnover rates of the chimeric isoenzymes and in particular the two C-terminal chimera, $(3^{209}4^{8})_2$ and $(3^{194}4^{23})_2$, suggests that egress of the product from the active site may be governed by the interactions of the rather flexible, meandering tail at the C-terminus with itself or other parts of the protein. Side-chain contacts of variable residues in exon 8 that are evident in the structure of isoenzyme 3–3 and may be important in this regard include van der Waals interactions between Y202 and H14, between L211 and Y40, between Q213 and the main-chain residues 114 and 116, and between S215 and W214 as well as hydrogen-bonding interactions between the hydroxyl groups of S209 and Y115 and between the hydroxyl group of S215 and the main-chain amide of I207. Whether product release remains the rate-limiting step in turnover of the chimeric isoenzymes is not known. If it still is in the case of $(3^{209}4^{8})_2$, then the quadruple mutation (L211M/Q213F/S215N/N216P) introduced at the C-terminus lowers the barrier for product release by as much as 5.3 kJ/mol, perhaps by increasing the flexibility of the tail.

Kinetics and Stereoselectivity in Michael Additions. The chimeric proteins described above represent an initial attempt to scan parts of the sequence of isoenzyme 4–4 in search of the structural elements that contribute to a particular catalytic characteristic of this enzyme, the efficiency and stereoselectivity toward α,β-unsaturated ketones. It is clear from the data in Tables II and III that the chimeric isoenzymes behave as unique catalysts that bear some resemblance to both of the parent isoenzymes. A comparison of the response of the two diastereomeric transition states for the addition of GSH to the enone substrates catalyzed by the two parent isoenzymes and the representative chimera is very informative with respect to the mechanistic basis of the stereoselectivity and catalytic efficiency of isoenzyme 4–4. The fact that the chimeric proteins, particularly those with the three mutations in exon 1, exhibit an isoenzyme 4–4-like stereoselectivity with little increase in catalytic efficiency indicates that the stereoelectronic basis of efficiency and selectivity is different and can be dissected. This view appears to be borne out in the linear free energy relationships observed with the two parents and $(4^{193}3^{198})_2$ toward this class of substrates.

The observed k_{cat}/K_m^{XPBO} is a composite of the rate constants (k_{cat}/K_m^{A} and k_{cat}/K_m^{B}) associated with attainment of the two diastereomeric transition states. It, as well as any linear free energy relationships associated with it, is a weighted average for the two parallel transition states in which the

[6] The rate constant for desorption of the product from the active site of isoenzyme 3–3 at pH 7.0 and 25 °C has been measured by stopped-flow techniques to be about 17 s^{-1}, which is clearly comparable to the turnover of 19 s^{-1} (W. W. Johnson and R. N. Armstrong, unpublished results).

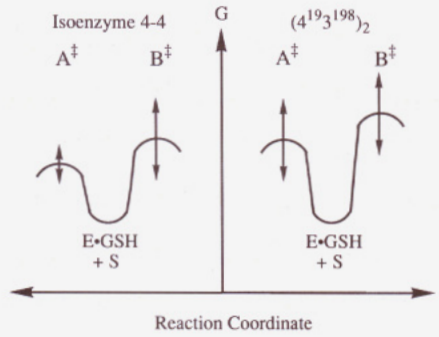

FIGURE 6: Relative free energies of activation for the transition states ($A^{\ddagger}$ and $B^{\ddagger}$) for the formation of the two diastereomeric products in the addition of GSH to **1** catalyzed by isoenzyme 4–4 and $(4^{19}3^{198})_2$. The relative heights of the activation barriers for the two enzymes are roughly normalized to one another using k_{cat}/K_m^{PBO}. The sensitivites of the transition states to the electronic effect of the substituent are represented by the double-headed arrows corresponding to the magnitudes of ρ_A and ρ_B.

transition state of lowest $\Delta G^{\ddagger}$ dominates. However, the dependence of the stereoselectivity of the enzyme-catalyzed reaction on σ can be used to determine if the two parallel transition states differ in their electronic character. For example, the dependence of $A^{\ddagger}$ (the transition state of lower $\Delta G^{\ddagger}$) on σ is much less than that for $B^{\ddagger}$ ($\rho_A = 0.78$ and $\rho_B = 1.74$) in the isoenzyme 4–4-catalyzed reaction (Kubo & Armstrong, 1989). This is illustrated in Figure 6 in which the magnitude of ρ for each transition state is shown as a vector imposed on the activation barrier perpendicular to the reaction coordinate. The lower sensitivity of $A^{\ddagger}$ to the electron-withdrawing ability of the substituent suggests that this particular transition state enjoys additional electronic stabilization contributed by the enzyme which accounts for the generally higher efficiency (k_{cat}/K_m^{XPBO}) of isoenzyme 4–4 toward the enone substrates.

The addition of GSH to enones **1**–**5** catalyzed by isoenzyme 3–3 and $(4^{19}3^{198})_2$ is more sensitive to the electronic effect of the para substituent, a fact that is consistent with the lower efficiency of these two enzymes as compared to isoenzyme 4–4. Unfortunately, the somewhat willy-nilly response of both the kinetics and stereoselectivity of isoenzyme 3–3 to the substituent makes it difficult to come to a quantitative understanding of the stereoelectronic effects that influence its catalytic character. However, it is clear that, to a first approximation, both transition states respond rather significantly to the electronic effect of the substituent such that $\rho_A \cong \rho_B \geq 1.2$, which is much larger than ρ_A for isoenzyme 4–4. Thus neither transition state is stabilized by isoenzyme 3–3 as effectively as $A^{\ddagger}$ is by isoenzyme 4–4.

The two most significant observations about the chimeric isoenzyme are the dependence of k_{cat}/K_m^{XPBO} and the independence of the stereoselectivity on σ. Clearly both transition states are very sensitive to the electron-withdrawing ability of the substituent and, more interestingly, that sensitivity is virtually the same as that of $B^{\ddagger}$ in the isoenzyme 4–4-catalyzed reaction illustrated by the broken line of Figure 3. This is a very obvious indication that neither transition state benefits from the same degree of electronic stabilization that $A^{\ddagger}$ realizes from isoenzyme 4–4. Furthermore, since $A^{\ddagger}$ and $B^{\ddagger}$ in the $(4^{19}3^{198})_2$-catalyzed reaction seem to be indistinguishable electronically, it is reasonable to conclude that the discrimination between the two is due to substituent-independent steric interactions with the active site. It may therefore be true that the molecular basis of the stereoselectivity of isoenzyme 4–4 is at least partly steric but with the superposition of a significant electronic stabilization of one of the two transition states.

Origins of the Catalytic Efficiency and Stereoselectivity. The three-dimensional structure of isoenzyme 3–3 offers no obvious clue to the structural basis for the differences in catalytic efficiency exhibited by isoenzymes 4–4 and 3–3 or the chimeric isoenzymes. Preliminary model-building exercises in which the enone is floated into the active site of the binary isoenzyme 3–3–GSH complex reveal no clear indication as to which mutatable side chains of isoenzyme 4–4 might be responsible for the electrostatic stabilization of $A^{\ddagger}$. Since the chimeric isoenzymes constructed in this work did not mimic the enhanced efficiency of the parent 4–4, no direct conclusions can be drawn other than the crucial residue(s) may lie outside variable regions 1 and 4. In any event, the differences in rate

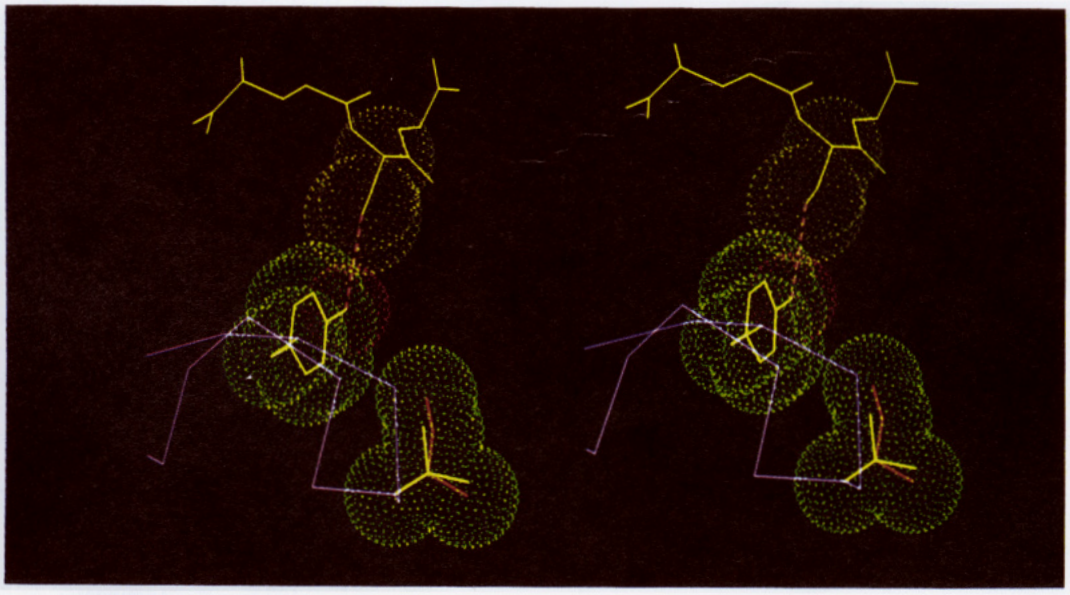

FIGURE 7: Stereoview of the relationship of the side chains of Y6, V9, and GSH in the active site of isoenzyme 3–3. The structure of GSH and the side chains of V9 and Y6 are shown in yellow along with the Cα trace for residues 4–15 in purple. The van der Waals volumes of the side chain of Y6 and the cysteine residue of GSH are shown as dot surfaces. The calculated position of the side chain of I9 is shown in red, and the calculated van der Waals surface is shown in green.

accelerations are only about a factor of 10, so the electrostatic differences between the active sites may be very subtle.

The N-terminal hybrids provide a clear, positive catalytic signal with respect to the origins of the stereoselectivity of the hybrids and, by implication, the parent isoenzyme 4–4 toward the enone substrates. One or more of the mutations in exon 1, namely, I3T, N8D, and V9I, seem to be responsible for the high degree of discrimination between the two diastereomeric transition states exhibited by these isoenzymes. However, when viewed in the context of the three-dimensional structure of isoenzyme 3–3, two of the mutations appear to be benign in this regard. For example, the I3T mutation is located on the solvent-exposed face of the β-sheet in the N-terminal domain of the protein and faces away from the active site (Figure 5). The side chain of N8, which is located in the turn connecting the first β-strand with the first α-helix, also faces away from the active site into solvent. Neither the I3T nor the N8D mutation is likely to have any significant consequence for the structure of the active site. In contrast, the *pro-S* methyl group of the side chain of V9 is located 6.4 Å from the sulfur of GS^- and is in van der Waals contact with the catalytically important residue Y6 (Liu et al., 1992), the hydroxyl group of which is hydrogen bonded to the thiolate of GS^- (Figure 7). The V9I mutation extends the *pro-S* arm of the side chain by a methylene group which must result in either movement of the side chain of Y6 or a rotation of the extended arm of the I9 away from Y6 and into the active site cavity. Although the former may be possible, the latter seems more likely. Molecular modeling of the V9I mutation into the structure of isoenzyme 3–3 indicates that one favored conformation of the side chain places the terminal methyl group of the S-arm of I9 about 1 Å closer to the sulfur of GS^- than to the *pro-S* methyl group of V9 (Figure 7). This added steric knob is the most probable cause of the altered stereoselectivity of the chimeric isoenzymes and may also contribute substantially to the stereoselectivity of isoenzyme 4–4.

Conclusions. Mechanistic and structural analysis of the functional properties of chimeric isoenzymes suggests that both the N- and C-terminal ends of isoenzymes 3–3 and 4–4 are directly involved in defining the catalytic character of GSH transferases from the mu class. The higher turnover numbers observed with chimeras in which the C-terminal variable region of subunit 3 is replaced with that of subunit 4 indicate that interaction of the flexible C-terminal tail with the N-terminal domain helps limit the rate of product release from the active site of isoenzyme 3–3 in nucleophilic aromatic substitution reactions. Modular mutants of the N-terminal variable region have allowed the rapid location of a residue at position 9 which is crucial in determining the stereoselectivity of the chimeras and, by implication, isoenzyme 4–4 toward phenylbutenones and arene oxides. Construction and analysis of other complementary chimeric isoenzymes and single-site mutants should help to confirm these conclusions and help to refine our understanding of the structural and mechanistic bases for catalytic diversity of the GSH transferases in the detoxification of xenobiotics.

ACKNOWLEDGMENT

The authors thank Dr. Cecil Pickett and Professor David Tu and their research groups for generously providing the original cDNA clones from which the expression vectors were constructed and William W. Johnson for help with the fluorescence titrations.

REFERENCES

Abramovitz, M., & Listowsky, I. (1987) *J. Biol. Chem. 262*, 7770–7773.
Armstrong, R. N. (1990) *Chem. Rev. 90*, 1039–1325.
Armstrong, R. N. (1991) *Chem. Res. Toxicol. 4*, 131–140.
Boehlert, C. C., & Armstrong, R. N. (1984) *Biochem. Biophys. Res. Commun. 121*, 980–986.
Chen, W.-J., Graminski, G. F., & Armstrong, R. N. (1988) *Biochemistry 27*, 647–654.
Cleland, W. W. (1979) *Methods Enzymol. 63*, 103–138.
Cobb, D., Boehlert, C., Lewis, D., & Armstrong, R. N. (1983) *Biochemistry 22*, 805–812.
Ding, G. J.-F., Lu, A. Y. H., & Pickett, C. B. (1985) *J. Biol. Chem. 260*, 13268–13271.
Ding, G. J.-F., Ding, V. D.-H., Rodkey, J. A., Bennett, C. D., Lu, A. Y. H., & Pickett, C. B. (1986) *J. Biol. Chem. 261*, 7952–7957.
Fujita, T., Iwasa, J., & Hansch, C. (1964) *J. Am. Chem. Soc. 86*, 5175–5183.
Graminski, G. F., Zhang, P., Sesay, M. A., Ammon, H. L., & Armstrong, R. N. (1989) *Biochemistry 28*, 6252–6258.
Hansch, C., & Leo, A. (1979) *Substituent Constants for Correlation Analysis in Chemistry and Biology*, Wiley, New York.
Ji, X., Zhang, P., Armstrong, R. N., & Gilliland, G. L. (1992) *Biochemistry* (preceding paper in this issue).
Kubo, Y., & Armstrong, R. N. (1989) *Chem. Res. Toxicol. 2*, 144–145.
Lai, H.-C., J., & Tu, C.-P. D. (1986) *J. Biol. Chem. 261*, 13793–13799.
Lai, H.-C., Grove, G., & Tu, C.-P. D. (1986) *Nucleic Acids Res. 14*, 6101–6114.
Lai, H.-C., J., Qian, B., Grove, G., & Tu, C.-P. D. (1988) *J. Biol. Chem. 263*, 11389–11395.
Liu, S., Zhang, P., Ji, X., Johnson, W. W., Gilliland, G. L., & Armstrong, R. N. (1992) *J. Biol. Chem. 267*, 4296–4299.
Mannervik, B., & Danielson, U. H. (1988) *CRC Crit. Rev. Biochem. 23*, 283–337.
Mannervik, B., Alin, P., Guthenberg, C., Jensson, H., Tahir, M. K., Warholm, M., & Jornvall, H. (1985) *Proc. Natl. Acad. Sci. U.S.A. 82*, 7202–7206.
Meyer, D. J., Coles, B., Pemble, S. E., Gilmore, K. S., Fraser, G. M., & Ketterer, B. (1991) *Biochem. J. 274*, 409–414.
Pickett, C. B., & Lu, A. Y. H. (1989) *Annu. Rev. Biochem. 58*, 743–764.
Tabor, S., & Richardson, C. C. (1989) *Proc. Natl. Acad. Sci. U.S.A. 86*, 4076–4080.
Tartof, K. D., & Hobbs, C. A. (1987) *Bethesda Res. Lab. Focus 9*, 12.
Zhang, P., & Armstrong, R. N. (1990) *Biopolymers 29*, 159–169.
Zhang, P., Graminski, G. F., & Armstrong, R. N. (1991) *J. Biol. Chem. 266*, 19475–19479.